



Contents lists available at ScienceDirect

Materials Science & Engineering A

journal homepage: www.elsevier.com/locate/msea

Effect of global constraint on the mechanical behavior of gradient materials

Jingran Yang^{a,b}, Le Xu^c, Hongliang Gao^a, Xingfu Li^a, Hongjiang Pan^a, Baipo Shu^a, Takamoto Itoh^c, Yuntian Zhu^{d,e,*}, Xinkun Zhu^{a,**}

^a Faculty of Materials Science and Engineering, Kunming University of Science and Technology, Kunming, Yunnan, 650093, China

^b City College, Kunming University of Science and Technology, Kunming, Yunnan, 650051, China

^c Department of Mechanical Engineering, College of Science and Engineering, Ritsumeikan University, Kusatsu-shi, Shiga, 525-8577, Japan

^d Department of Materials Science and Engineering, City University of Hong Kong, China

^e Mechanical Behaviour Division of Shenyang National Laboratory for Materials Science, City University of Hong Kong, China

ARTICLE INFO

Keywords:

Global constraint

Gradient structure

Mechanical properties

HDI effect

Double-sided

Single-sided

ABSTRACT

The gradient structured (GS) samples studied here consists of gradient layer (s) with grain size gradient and a coarse-grained (CG) layer. Gradient materials have been found to have superior mechanical properties due to the hetero-deformation induced (HDI) strengthening and strain hardening. However, the effect of the interaction between the GS layer and the CG layer on the mechanical properties of the gradient materials remains to be studied. In this paper, single-sided GS Cu and double-sided GS Cu plates were prepared by surface mechanical attrition treatment (SMAT) on one side and both symmetrical sides respectively. It is found that GS samples have higher yield strength than CG samples, and the Cu samples with double-sided GS has a uniform elongation comparable to CG Cu. In addition, the global mutual constraint among different GS layers affect the mechanical behavior of gradient materials, which is revealed in the comparative study of double-sided and single-sided GS Cu. Specifically, the double-sided GS Cu exhibit higher yield strength and ductility than the single-sided GS Cu, because the former is better constrained. This study demonstrates that in addition to the local structural gradient, the symmetric constraint produce more effective HDI effect to enhance the mechanical properties. The global mutual constraints of GS layers played a positive role in producing superior mechanical properties.

1. Introduction

In the field of metallic materials, there is a tireless effort to improve strength while maintaining ductility. In general, nanocrystalline materials tend to exhibit lower ductility, although the strength is several times higher than their CG counterparts [1–3]. The traditional theory of fine grain strengthening follows the principle of Hall-Petch, that is, the grain refinement can improve the strength of materials. However, the ductility is usually decreases with increasing strength [4].

In recent years, it has been found that GS can produce a superior combination of strength and ductility that is not accessible to homogeneous structures [5]. The superior mechanical properties have been attributed to the hetero-deformation induced strengthening and strain hardening [6–9]. The HDI stress is produced by the piling up of geometrically necessary dislocations (GNDs), which is needed to accommodate the strain gradient during the deformation of GS. In other words, the GS produces extra strengthening and strain hardening during

tensile deformation. It was also suggested that the two-dimensional stresses are evolved from the applied uniaxial stress during tensile deformation due to the global constraint in the double-sided GS sample [5]. The multi-axial stresses are assumed to activate more slip systems to effectively increase the dislocation density, causing dislocation hardening [10,11]. However, it is not clear if this effect is significant enough to affect the mechanical behavior and the HDI strain hardening. There are some unique extra strengthening effects, which provided the high yield strength meanwhile retained good ductility in GS metals [12–15]. Therefore, the source of these effects and the interaction between GS layer and CG matrix need to be further explored.

In this study, the pure copper with the single-sided GS and the double-sided GS were prepared by SMAT. We studied the effect of different constraint conditions on the mechanical properties of GS materials. (The synergetic strengthening effect compared with the rule-of-mixtures (ROM) [16] and the HDI stress strengthening by the Bauschinger effect test.) In addition, the difference in mechanical properties

* Corresponding author. Mechanical Behaviour Division of Shenyang National Laboratory for Materials Science, City University of Hong Kong, China.

** Corresponding author.

E-mail addresses: y.zhu@cityu.edu.hk (Y. Zhu), xk.zhu@hotmail.com (X. Zhu).

<https://doi.org/10.1016/j.msea.2021.141963>

Received 17 May 2021; Received in revised form 14 August 2021; Accepted 21 August 2021

Available online 21 August 2021

0921-5093/© 2021 Elsevier B.V. All rights reserved.

between samples with double-sided GS Cu and single-sided GS Cu were further studied using finite element simulation (FEM). The results of this study provide insight in the design of the microstructure in nanocrystalline metal materials.

2. Experimental procedure

The starting material Cu(99.9% purity) was vacuum annealed at 650 °C for 2 h to produce a uniform CG structure. The SMAT device (in Fig. 1a) consisted mainly of a vibration generator and a treatment chamber placing the balls as well as holding the sample. The surface of the annealed copper plate was continuously struck at high velocity from different angles by the 108 balls with a diameter of 8 mm (see Fig. 1b), and SMAT processed at room temperature for 15 min, which promoted the refinement of surface grains. It have obtained two types of samples, the single-sided GS Cu was produced by SMAT treatment on one side of the copper plate with thicknesses of 1.5 mm, 2 mm, and 2.5 mm (see Fig. 2a); the double-sided GS Cu was produced by SMAT treatment on both symmetrical sides of the copper plate with thicknesses of 3 mm, 4 mm, 5 mm (see Fig. 2c). We define the thickness of GS area as l and the total thickness of samples as L . The volume fractions of the corresponding two types of GS samples (see Fig. 2b) are the same for comparison.

Dog-bone shaped tensile samples (see Fig. 2a and c) were cut from the SMAT-processed plates by wire-electrode cutting, except for the sample thickness the geometry dimension of double-sided GS tensile sample was consistent with that of single-sided GS. Uniaxial tensile test and loading-unloading-reloading (LUR) experiment were performed at room temperature using a SHIMADZU Universal Tester, with a maximum load of 100 KN and the quasi-static strain rate of $5.0 \times 10^{-4} \text{ s}^{-1}$. The sample was stretched and deformed along the elongation direction in Fig. 2c. At least three tensile tests were conducted under each testing condition to ensure the reproducibility of the stress-strain curves. The LUR tests was set strain points of 1%, 2%, 3%, 4%, 5%, 6%, 7%, 8%, 9%, 10%. At each strain, the sample was unloaded in a load-control mode to 20 N at an unloading rate of 600 N min^{-1} , followed by reloading back to the level of applied load prior to unloading. The HDI stress was calculated from the measured of the LUR stress-strain curve.

The cross-sectional hardness of SMAT samples was measured by Vickers microhardness tester with a load of 0.49 N, a dwell time of 15 s, and a distance between adjacent indentations of 20 μm . The Vickers microhardness value was calculated according to the formula:

$$HV = \frac{2P \sin(\frac{\alpha}{2})}{d^2} = 1.854 \frac{P}{d^2} \quad (1)$$

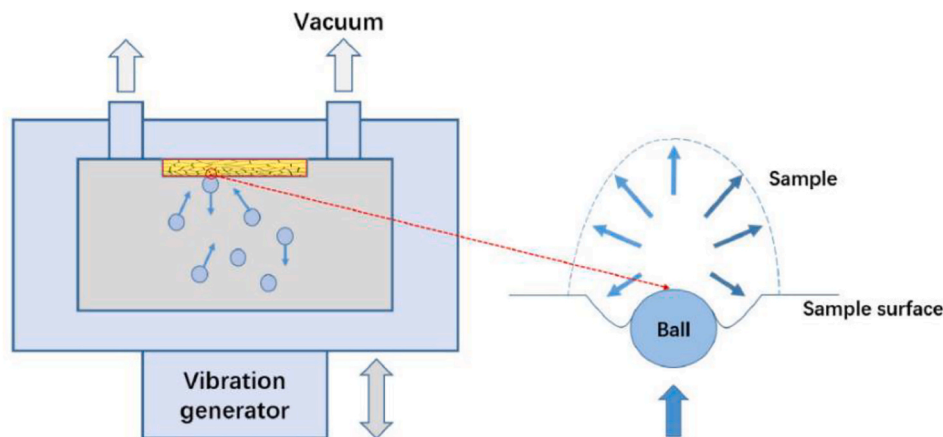


Fig. 1. (a) Schematic illustration of the SMAT device. (b) The plastic deformation in the surface layer caused by the repeated impact of the flying balls on the sample surface in multiple directions [17].

Where HV is Vickers hardness value, d is the diagonal length of the indentation, P is the load value and $\alpha = 136^\circ$ is the angle between the two opposite faces of the pyramid indenter. In addition, the hardness sampling area of the nanoindentation test (KLA-iMicro) covered the surface of the sample to the coarse-grained area. The nanoindentation experiment used an applied load of 30 mN for each hardness point. On the cross section of the sample, a hardness point was made every 30 μm from the surface to the core, 30 points in each line, and 30 lines were extended in the direction perpendicular to the cross section, a total of 900 points form a nano-hardness-point matrix.

3. Results and discussion

3.1. Microhardness and gradient structure

After the SMAT treatment, grains in the surface layer of Cu samples were refined, while the grains in the center layer remained coarse. A hardness gradient was formed from the surface to the center. As shown in Fig. 3a, the value of microhardness gradually decreasing from the SMAT surface to the interior of the sample. The cross-sectional hardness was determined by averaging the value of 6 indentations at each depth of the GS and CG area in Fig. 3a. After 350 μm depth, the microhardness curve become flat, with values close to that of the annealed Cu. The microhardness gradients of the single-sided GS Cu and the double-sided GS Cu is the same because of their identical processing. The hardness curve in Fig. 3a has been divided into three areas, marked as A, B and C. The author defines that the A and B areas are the GS layers, and from the C area to the core of the sample is CG layer. The GS layer thickness (l) is about the same (300 μm) on all samples due to same SMAT treatment time as well.

The area of 300 $\mu\text{m} \times 300 \mu\text{m}$ from the surface to the center was measured by the nanoindentation. Fig. 3b shows that the hardness of GS sample has changed from the surface to the core. With the increasing of the depth from the surface to the core, the red area is the hardness of the sample surface, the part between the red and blue areas is the gradient transition stage and the blue area is considered as the hardness value of CG. Fig. 3 indicates that the single-sided and double sided samples have comparable hardness gradients from the surface to the core. Generally, the nanoindentation value is higher than the microhardness value. The main reason for the inconsistent was that the methods of calculating hardness value were different [18].

3.2. Mechanical properties

Engineering tensile stress-strain curves of different samples are shown in Fig. 4a and the tensile properties are summarized in Table 1.

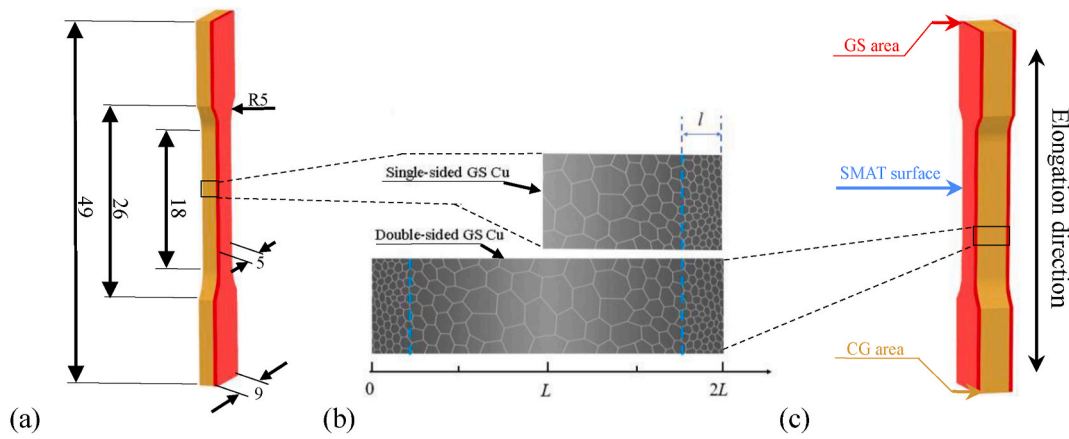


Fig. 2. (a) The geometry and size of the tensile sample with the single-sided GS. (b) Schematic illustration of the single-sided GS and the double-sided GS the samples processed by SMAT. (c) The geometry of the double-sided GS sample. The position of SMAT surface, the GS area and CG area on the tensile sample, and the elongation direction of the uniaxial tensile test.

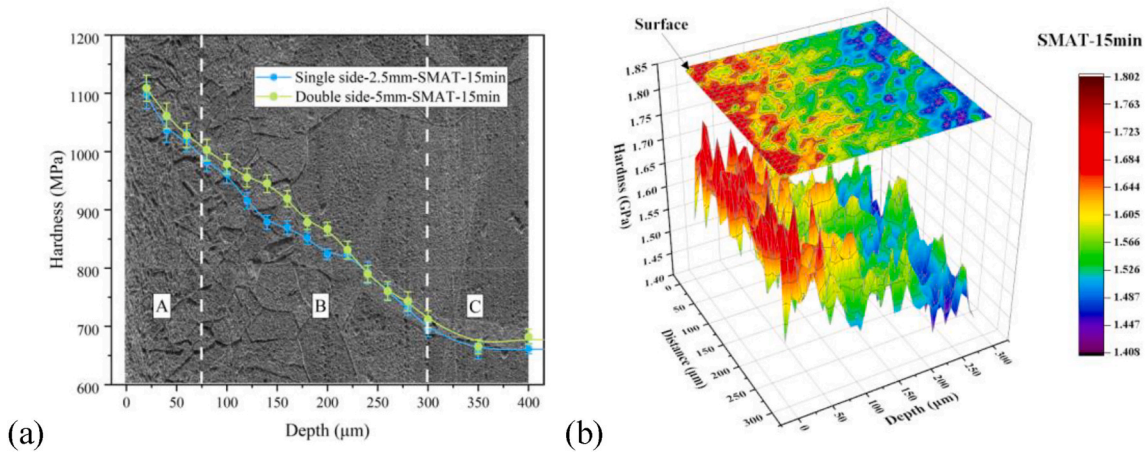


Fig. 3. (a) The microhardness values imposed on the optical image of the single-sided GS and double-sided GS Cu; (b) The nanoindentation hardness distribution from surface to core of the GS Cu.

The thickness of GS layer is about 300 μm for all samples because of the same SMAT time. The ratio of the thickness of GS layer to the thickness of different samples is also the volume fraction of the GS layer. The yield strength of the GS samples with GS layer and CG layer is more than three times that of the CG sample. At the same time, the uniform elongation of double-sided GS Cu was slightly lower than that of CG sample. It could be seen in Fig. 4b that the yield strength and the uniform elongation of double-sided GS Cu are higher than those of the single-sided GS Cu even though they have the same volume fraction of GS layers.

According to the strain hardening rate ($\theta = d\sigma/d\epsilon$) curves (Fig. 4c and d), the curves of double-sided GS Cu are not monotonously reduced as the strain increases. When the true strain is in the range of 0.02–0.04, the curves went up, which is attributed to the hetero-deformation induced (HDI) hardening [7]. The multiaxial stress state of the double-sided GS with global mutual constraint would activate more slip systems, which make it easier for dislocations to interact and entangle with each other to bring about the observed dramatic hardening rate up-turn [9]. Compared with the strain hardening curve of single-sided GS Cu, the curve of double-sided GS Cu is retained the strain hardening better (red arrow in Fig. 4d), which indicates that the strain hardening effect of double-sided GS Cu is stronger than that of single-sided GS Cu. The red dots at the intersection of the strain hardening rate and the true stress-strain curve in Fig. 4d, it could be seen that the necking of double-sided GS Cu is significantly later than that of single-sided GS Cu, which means that double-sided GS Cu have higher

ductility than single-sided GS Cu.

3.3. Synergetic strengthening and HDI strengthening

It can be found from Fig. 4a that the yield strength of GS Cu increases with the increase of GS layer volume fraction. In order to investigate this observation, we first calculate the yield strength of CG and GS Cu using rule of mixtures (ROM) [19]:

$$\sigma_{ROM} = V_{GS}\sigma_{GS} + (1 - V_{GS})\sigma_{CG} \quad (2)$$

The σ_{ROM} , represent the calculated yield strength of the whole sample, σ_{GS} is the yield strength of GS layer in 0.2% plastic strain, σ_{CG} represent the yield strength of CG Cu, and V_{GS} is the volume fraction of the GS layers. According to the above formula, the higher the volume fraction of GS layer in the material, the higher the overall yield strength. Fig. 5a shows a typical engineering stress-strain curve of the CG Cu and double-sided GS Cu with GS layer volume fraction of 15%. As shown, the GS sample has a higher yield strain than the CG sample. Consequently, a modified ROM equation needs to be used [9]:

$$\sigma_{ROM}^{mod} = V_{GS}\sigma_{GS} + (1 - V_{GS})\sigma'_{CG} \quad (3)$$

where the σ'_{CG} (see Fig. 5a) can be calculated by:

$$\sigma'_{CG} = \sigma_{CG} + \Delta\sigma \quad (4)$$

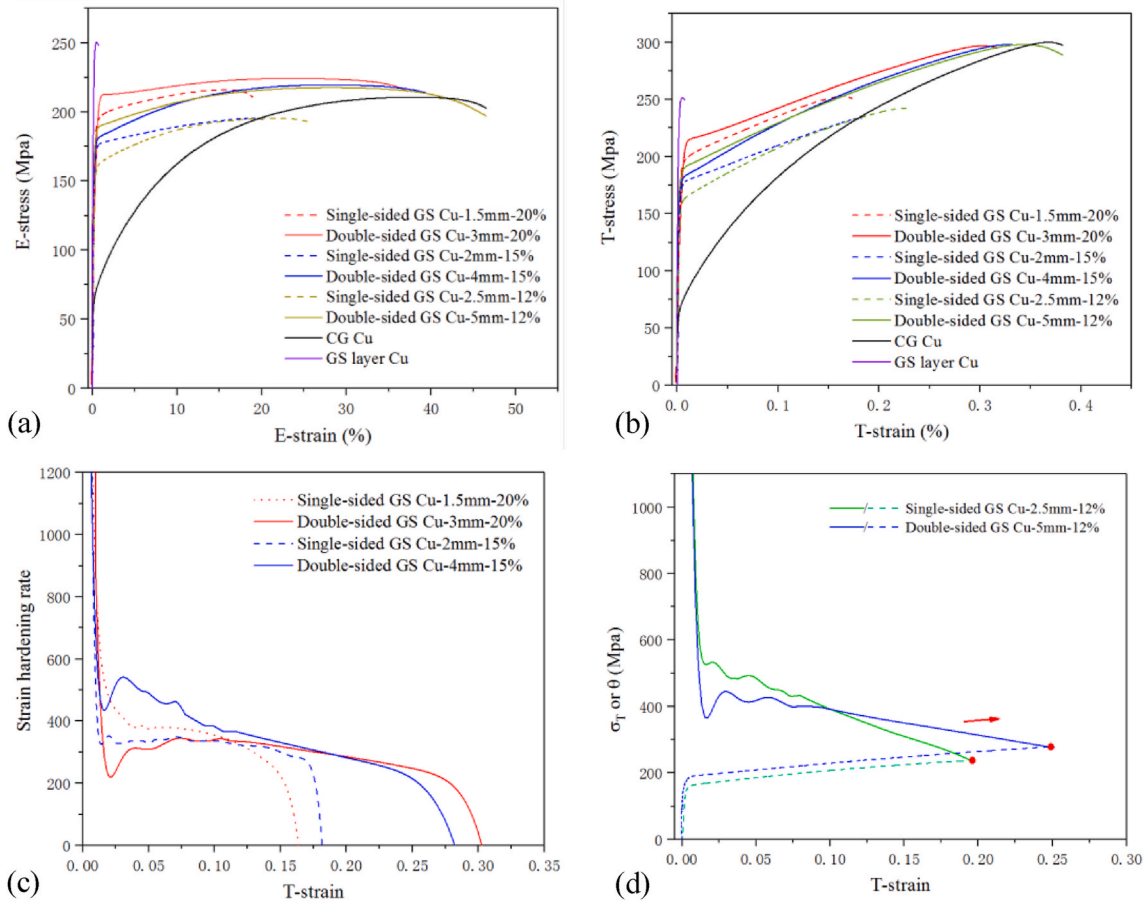


Fig. 4. (a) Tensile engineering stress-strain curve, including the CG Cu sample and the GS Cu samples with different thickness and different GS layers volume fraction. (b) The true stress-strain curves, including the CG Cu sample and the GS Cu samples with different thickness and different GS layers volume fraction. (c) The strain hardening rate curves of samples with GS layer volume fraction equals to 20% and GS layer volume fraction equals to 15%. (d) The strain hardening rate curves and true stress-strain curves of samples with GS layer volume fraction equals to 12%.

Table 1

The tensile properties of single-sided GS Cu and double-sided GS Cu under different volume fractions of GS layer and different sample thickness.

Type of GS Cu	Sample thickness (mm)	Volume fraction of GS layer (%)	YS (MPa)	UE (%)
Single-sided GS Cu	2.5	12	154	21.5
double-sided GS Cu	5		170	28.2
Single-sided GS Cu	2	15	160	19.1
double-sided GS Cu	4		174	27.9
Single-sided GS Cu	1.5	20	184	15.6
double-sided GS Cu	3		207	23.3

YS-yield strength; UE-uniform elongation.

The σ_{ROM}^{mod} represents the modified value of yield strength of the whole sample. It can be seen from Fig. 5b that the experimentally measured yield strength values of the double-sided and single-sided GS Cu are much higher than the corresponding values calculated by the modified ROM, which indicates a strong synergetic strengthening by the gradient structure. At the early stage of GS Cu tensile strain, the central CG layer deforms plastically, while the GS layer still deform elastically. The plastically deforming central layer has an apparent Poisson's ratio close to 0.5 to maintain a constant volume, while Poisson's ratio in the GS

layer is close to 0.3 [9]. The difference of Poisson's ratio lead to strain gradient and plastic incompatibility between GS layer and CG layer. The plastic incompatibility lead to the transformation from uniaxial stress to multi-axial stress, which promote the interaction of dislocations and the continuous accumulation of the GNDs [9]. The accumulation of these GNDs can produce extra strengthening effect during deformation which leads to the actual yield strength much higher than the modified ROM calculation results [8].

Furthermore, on the basis of ROM theory, the σ_{ROM}^{mod} of double-sided GS Cu should be consistent with that of single-sided GS Cu with the same volume fraction. (Inset of Fig. 5b, both of the curves are almost coincident.) The synergetic of yield strength values about two kinds of GS Cu can be calculated by the following formulas:

$$\sigma_{S-synergetic} = \sigma_{Single} - \sigma_{ROM}^{mod} \quad (5)$$

$$\sigma_{D-synergetic} = \sigma_{Double} - \sigma_{ROM}^{mod} \quad (6)$$

The $\sigma_{S-synergetic}$ and $\sigma_{D-synergetic}$ represent the difference between the experimental results of yield strength of single-sided and double-sided GS Cu with the modified ROM calculation results respectively. Through the calculation of the above formula, in the case of the same volume fraction, the $\sigma_{D-synergetic}$ of double-sided GS Cu (blue dotted curve) have a higher synergetic strengthening value than the $\sigma_{S-synergetic}$ of the single-sided GS Cu (red dotted curve) in Fig. 5b. This difference originates from the different global constraint in the single-sided and double-sided Cu, which affects the generation of the HDI stress [7]. As shown in Fig. 5c, the curves of double-sided GS Cu (solid lines) is always

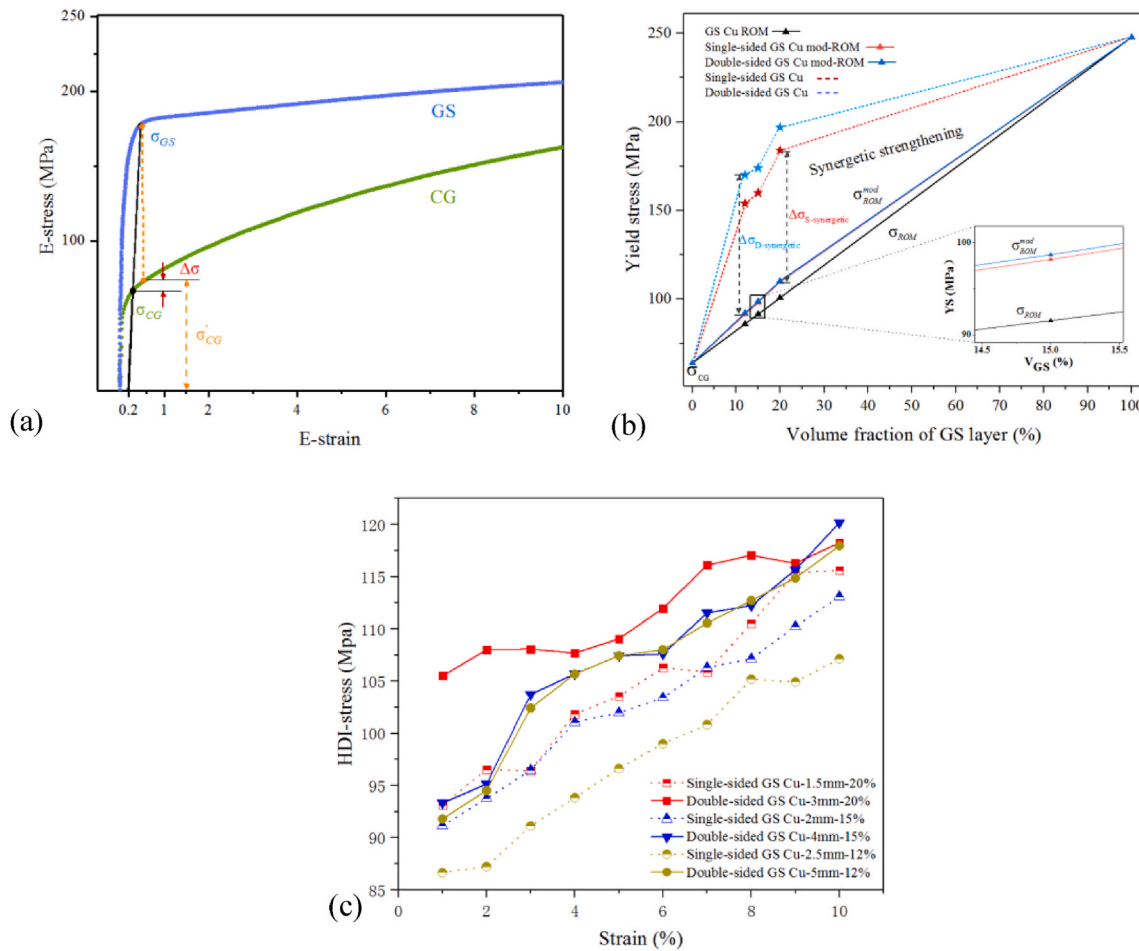


Fig. 5. (a) Schematic illustration of the corrected σ'_{CG} in engineering stress-strain curves of CG and double-sided GS Cu-4mm-15%; (b) The curves of yield strength include the double-sided and single-sided GS Cu actual value (blue and red dotted lines respectively), the ROM calculation results (black solid line), and the modified ROM calculation results of the double-sided and single-sided GS Cu (blue and red solid lines respectively). The curves in the black box of the figure are enlarged into illustration; (c) The HDI stress curves of GS Cu with various thicknesses, the HDI stress curves of the single-sided GS Cu is dotted lines, and curves of the double-sided GS Cu is solid lines. (For interpretation of the references to colour in this figure legend, the reader is referred to the Web version of this article.)

higher than that of the corresponding single-sided GS Cu (dotted lines), which leads to the higher yield strength on double-sided GS Cu [20–22]. It can be reasonably assumed that the double-sided Cu sample has a better mutual constraint among the different layers, and produces different stress states, which led to the higher HDI stresses. More studies are needed to probe this issue.

3.4. Finite element simulation and analysis

Finite element simulation could further study the influence of global mutual constraining on the mechanical behavior of GS material. The commercial software MARC [23] was used to calculate the stress and strain distributions of GS materials. The GS was considered to be a multilayered structure which was divided into five layers through transversal direction (as the X direction) as shown in Fig. 6a. We assume that the deformation behavior of the material was the same inside each layer, but the different between different layers (Fig. 6b). A multi-linear kinematic hardening rule also shown in Fig. 6b was used to calculate the material deformation behavior in FEM. The isotropic hypothesis and small strain analysis had been conducted. The Poisson's ratio and elastic modulus of five layers were equal to 0.33 and 125000 GPa. Plane stress condition and four-node type element [24] were conducted in finite element simulations and the boundary conditions of single-sided and double-sided models were shown in Fig. 6a. The length of the element along thickness direction was set to be 0.1 mm, and that along

longitudinal direction is set to be a gradient increase which started from 0.05 mm to 0.45 mm 2500 elements and 2626 nodes were used in FEM. The bottom edges of single-sided GS and double-sided GS were applied with symmetrical constraints ($D_Y = 0$, and $R_Z = 0$) in which movement in tensile direction (as the Y direction) and in-plane rotation were not allowed. For the single-sided GS, the bottom right corner of edge was constrained with the movement in X direction ($D_X = 0$). Herein, fixing one node along X-direction was to avoid rigid body translation in the simulation. However, for double-sided GS, the right edge was applied with mutual constraints ($D_X = 0$, and $R_Z = 0$) as load and structure were symmetrical. When applying displacement control, an implicit constraint was generated, that was, the relative deformation between the layers was cancelled out. Then, the displacements or strains among different layers could be the same, so the relative constraints between the layers could not be obtained. Therefore, Edge loaded with same magnitude F were applied on upper edge of single-sided GS and double-sided GS models.

The FEM produce similar stress-strain curves as compared with experiment results in Fig. 7a and Fig. 7b, in which the yield strength of double-sided GS is higher than that of single-sided GS. It should be noted that the stress-strain curves of FEM for double-sided and single-sided are calculated on the basis of average value of stress and strain of nodes on Fig. 7c. We consider that the calculated average value of stress and strain are equivalent to the stress and strain obtained from uniaxial tension tests. The distribution of stress and strain at yielding point (as 0.2%

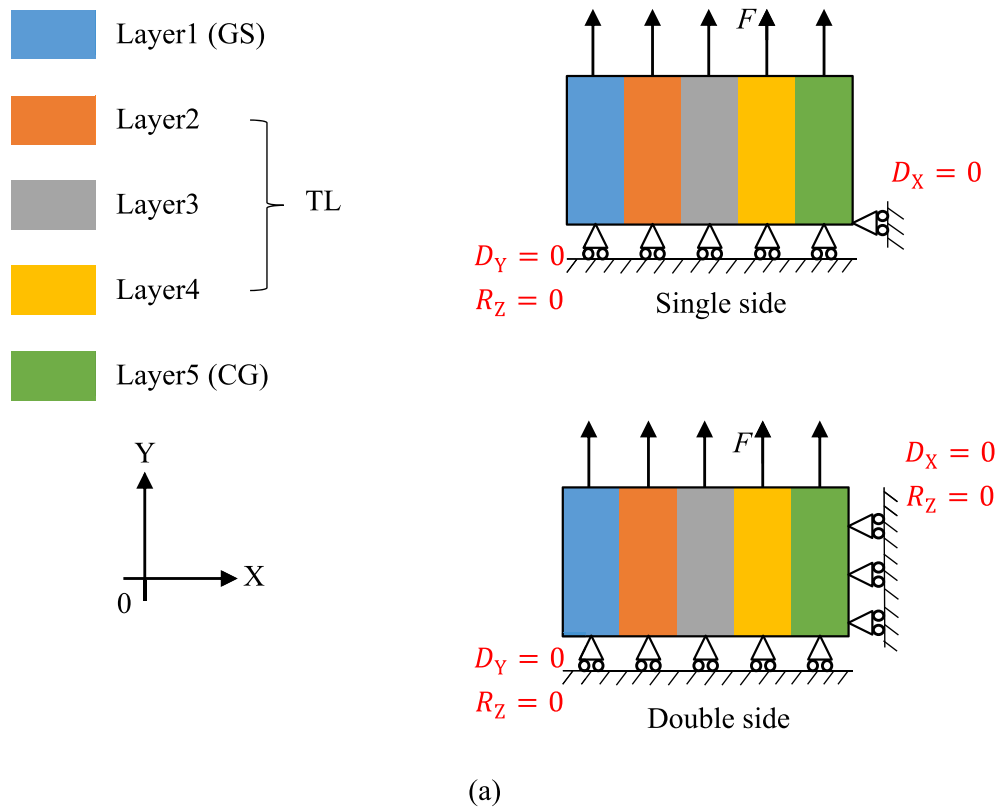


Fig. 6. Schematic FEM model showing the gauge section of tensile sample: (a) layer configuration and boundary conditions; (b) material deformation behavior for each layer. The yield strengths of Layer1 and Layer5 are determined from the test results, and equal to 250 MPa and 70 MPa, respectively.

average strain) is presented in Fig. 7c for double-sided and single-sided specimens. It is found that the strain of each layer of the double-sided GS is similar, while the strain distribution of each layer of the single-sided GS is different. This is mainly due to the symmetric constraint on the double-sided GS and the lack of constraining on the other side of the single-sided GS. As a result, the strain of the single-sided GS is mostly concentrated in the outer CG layers, so that the inner GS layer had little strain. When the average strain of the material is around 0.2%, FEM (Fig. 7d) shows that the stress distribution from GS layer to CG layer decreases stepwise along the thickness direction due to global mutual

restraint on double-sided GS Cu. However, because of no constraint on the other side of single-sided GS Cu, the strain in the CG layer during deformation is higher than that in the GS layer. Since, the material as a whole is slightly inclined to the fine-grained side, it has caused the CG layer to be in a state of compressive stress (negative value of stress), where the yield strength exhibited is lower than that of the double-sided GS. From the FEM shows that the yield strength of single-sided GS Cu are lower than those of double-sided GS Cu due to the compressive stress state and uneven strain distribution in the deformation process. Obviously, the global mutual constraint can effectively optimize the

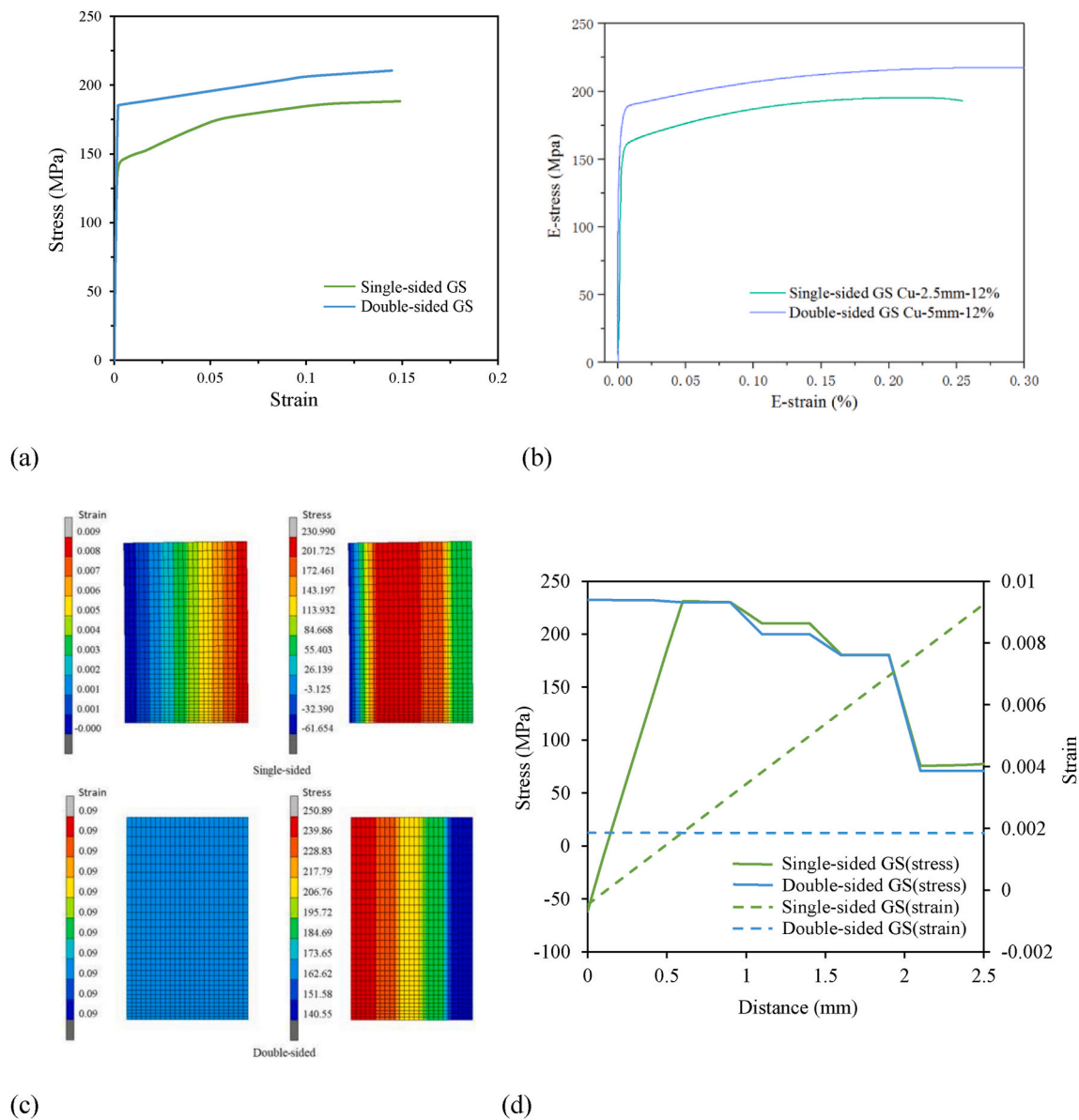


Fig. 7. Tensile stress-strain curves and stress distributions generated by finite element simulations: (a) FEM stress-strain curves of double-sided and single-sided samples; (b) engineering stress-strain curves of double-sided and single-sided samples; (c) the finite element mesh and the distribution of stress and strain for double-sided and single-sided specimen obtained by FEM at yielding point; (d) stress and strain variations along thickness direction on 0.2% average strain.

mechanical properties of GS materials.

4. Conclusions

In summary, the single-sided and double-sided GS Cu with different constraining conditions on CG central layer are obtained by SMAT process. The major conclusions drawn from this study are as follows:

- 1) The mechanical properties of the double-sided GS Cu is significantly better than that of the single-sided CG Cu. The yield strength and the uniform elongation of double-sided GS Cu are higher than that of the single-sided GS Cu. (The same behavior has been observed in 12%, 15% and 20% volume fraction of GS layer.)
- 2) Comparing to the single-sided GS Cu, the global mutual constraint in double-sided GS Cu may produce different stress states. This lead to higher HDI stress strengthening.
- 3) The double-sided GS Cu with mutual-constraint can delay strain localization, which helps uniformly distribute stress and avoids

strain concentration. The uniform distribution of stress and strain could improve the ductility of the sample, which is verified by FEM. These conclusions provide a new perspective for the study of mechanical properties of gradient structure metal materials.

Data availability statement

The processed data required to reproduce these findings cannot be shared at this time due to technical or time limitations.

CRediT authorship contribution statement

Jingran Yang: Investigation, Methodology, Data curation, Writing – original draft. **Le Xu:** Conceptualization, Formal analysis. **Hongliang Gao:** Investigation, Data curation. **Xingfu Li:** Validation, Visualization. **Hongjiang Pan:** Supervision, Project administration, Funding acquisition. **Baipo Shu:** Resources, Investigation. **Takamoto Itoh:** Supervision, Project administration. **Yuntian Zhu:** Writing – review & editing,

Funding acquisition. **Xinkun Zhu:** Writing – review & editing, Supervision, Funding acquisition.

Declaration of competing interest

The authors declare that they have no known competing financial interests or personal relationships that could have appeared to influence the work reported in this paper.

Acknowledgments

The authors would like to acknowledge financial support by the National Natural Science Foundation of China (NSFC) under Grants No. 51664033, No. 51911540072, No. 51861015, and 2019 Japan Society for the Promotion of Science JSPS/NSFC Bilateral Joint Research Project. The authors were supported Apply Basic Research of Foundation of Yunnan Province for Young Scientists (Grant No. 202001AU070081). YTZ acknowledge the supports of the Hong Kong Institute of Advance Studies and the National Science Foundation of China (Grants No.51931003) and the Hong Kong Research Grants Council (GRF 11214121). LX acknowledge the supports by the China Scholarship Council (Grants No. CSC201906745018).

References

- [1] M.A. Meyers, A. Mishra, D.J. Benson, Mechanical properties of nanocrystalline materials, *Prog. Mater. Sci.* 51 (2006) 427–556, <https://doi.org/10.1016/j.pmatsci.2005.08.003>.
- [2] Y.M. Wang, E. Ma, Three strategies to achieve uniform tensile deformation in a nanostructured metal, *Acta Mater.* 52 (2004) 1699–1709, <https://doi.org/10.1016/j.actamat.2003.12.022>.
- [3] P.G. Sanders, J.A. Eastman, J.R. Weertman, Elastic and tensile behavior of nanocrystalline copper and palladium, *Acta Mater.* 45 (1997) 1359–6454, [https://doi.org/10.1016/S1359-6454\(97\)00092-X](https://doi.org/10.1016/S1359-6454(97)00092-X).
- [4] E.O. Hall, The deformation and ageing of mild steel: III discussion of results, *Proc. Phys. Soc. B* 64 (1951) 747–753.
- [5] X. Wu, P. Jiang, L. Chen, F. Yuan, Y.T. Zhu, Extraordinary strain hardening by gradient structure, *Proc. Natl. Acad. Sci. U. S. A.* 111 (2014) 7197–7201, <https://doi.org/10.1073/pnas.1324069111>.
- [6] Y.T. Zhu, K. Ameyama, P.M. Anderson, I.J. Beyerlein, H.J. Gao, H.S. Kim, E. J. Lavernia, S.N. Mathaudhu, H. Maghrabi, R.O. Ritchie, N. Tsuji, X.Y. Zhang, X. L. Wu, Heterostructured materials: superior properties from hetero-zone interaction, *Mater. Res. Lett.* 9 (2021) 1–30, <https://doi.org/10.1080/21663831.2020.1796836>.
- [7] Y. Zhu, X. Wu, Perspective on hetero-deformation induced (HDI) hardening and back stress, *Mater. Res. Lett.* 7 (2019) 393–398, <https://doi.org/10.1080/21663831.2019.1616331>.
- [8] M.X. Yang, Y. Pan, F.P. Yuan, Y.T. Zhu, X.L. Wu, Back stress strengthening and strain hardening in gradient structure, *Mater. Res. Lett.* 4 (2016) 145–151, <https://doi.org/10.1080/21663831.2016.1153004>.
- [9] X.L. Wu, P. Jiang, L. Chen, J.F. Zhang, F.P. Yuan, Y.T. Zhu, Synergetic strengthening by gradient structure, *Mater. Res. Lett.* 2 (2014) 185–191, <https://doi.org/10.1080/21663831.2014.935821>.
- [10] D.V. Wilson, P.S. Bate, Influences of cell-walls and grain-boundaries on transient responses of an IF steel to changes in strain path, *Acta Metall. Mater.* 42 (1994) 1099–1111, [https://doi.org/10.1016/0956-7151\(94\)90127-9](https://doi.org/10.1016/0956-7151(94)90127-9).
- [11] J. Robert, Asaro, Micromechanics of crystals and polycrystals, *Adv. Appl. Mech.* 23 (1983) 1–115, [https://doi.org/10.1016/S0065-2156\(08\)70242-4](https://doi.org/10.1016/S0065-2156(08)70242-4).
- [12] K. Lu, Making strong nanomaterials ductile with gradients, *Science* 345 (2014) 1455–1456, <https://doi.org/10.1126/science.1255940>.
- [13] I.A. Ovid'ko, R.Z. Valiev, Y.T. Zhu, Review on superior strength and enhanced ductility of metallic nanomaterials, *Prog. Mater. Sci.* 94 (2018) 462–540, <https://doi.org/10.1016/j.pmatsci.2018.02.002>.
- [14] X. Liu, K. Wu, G. Wu, Y. Gao, L. Zhu, Y. Lu, J. Lu, High strength and high ductility copper obtained by topologically controlled planar heterogeneous structures, *Scripta Mater.* 124 (2016) 103–107, <https://doi.org/10.1016/j.scriptamat.2016.07.003>.
- [15] X. Yang, X. Ma, J. Moering, H. Zhou, W. Wang, Y. Gong, J. Tao, Y. Zhu, X. Zhu, Influence of gradient structure volume fraction on the mechanical properties of pure copper, *Mater. Sci. Eng., A* 645 (2015) 280–285, <https://doi.org/10.1016/j.msea.2015.08.037>.
- [16] Y.F. Wang, C.X. Huang, M.S. Wang, Y.S. Li, Y.T. Zhu, Quantifying the synergetic strengthening in gradient material, *Scripta Mater.* 150 (2018) 22–25, <https://doi.org/10.1016/j.scriptamat.2018.02.039>.
- [17] K. Lu, J. Lu, Nanostructured surface layer on metallic materials induced by surface mechanical attrition treatment, *Mater. Sci. Eng., A* 375–377 (2004) 38–45, <https://doi.org/10.1016/j.msea.2003.10.261>.
- [18] L. Qian, M. Li, Z. Zhou, H. Yang, X. Shi, Comparison of nano-indentation hardness to microhardness, *Surf. Coating. Technol.* 195 (2–3) (2005) 264–271, <https://doi.org/10.1016/j.surfcoat.2004.07.108>.
- [19] K.K. Chawla, On the applicability of the "rule-of-mixtures" to the strength properties of metal-matrix composites, *Revista Brasileira de Física* 4 (1974) 411–418.
- [20] Z. Yin, X. Yang, X. Ma, J. Moering, J. Yang, Y. Gong, Y. Zhu, X. Zhu, Strength and ductility of gradient structured copper obtained by surface mechanical attrition treatment, *Mater. Des.* 105 (2016) 89–95, <https://doi.org/10.1016/j.matdes.2016.05.015>.
- [21] T.H. Fang, W.L. Li, N.R. Tao, K. Lu, Revealing extraordinary intrinsic tensile plasticity in gradient nano-grained copper, *Science* 331 (6024) (2011) 1587–1590, <https://doi.org/10.1126/science.1200177>.
- [22] S.S. Chakravarthy, W.A. Curtin, Stress-gradient plasticity, *Proc. Natl. Acad. Sci. U. S. A.* 108 (38) (2011) 15716–15720, <https://doi.org/10.1073/pnas.1107035108>.
- [23] MSC Software Corporation, Marc Student Edition, MSC Software Corporation, Newport Beach, California, 2020.
- [24] MSC Software Corporation, Marc Student Edition: Element Library, B, MSC Software Corporation, Newport Beach, California, 2020.